Hindawi
Journal of Sensors
Volume 2022, Article ID 4016357, 18 pages
https://doi.org/10.1155/2022/4016357

Research Article

Experimental Study on Overlying Strata Movement Characteristics and Distributed Optical Fiber Characterization of Stope

Jing Chai,[1,2] Zhicheng Tian,[1] Yibo Ouyang,[1] Yongliang Liu,[1] Dingding Zhang,[1,2] and Jianfeng Yang[1,2]

[1]*School of Energy Science and Engineering, Xi'an University of Science and Technology, Xi'an, Shaanxi 710054, China*
[2]*Key Laboratory of Western Mine Exploitation and Hazard Prevention, Ministry of Education, Xi'an, Shaanxi 710054, China*

Correspondence should be addressed to Zhicheng Tian; zctianzc@163.com and Yibo Ouyang; 17629014025@163.com

Received 28 August 2022; Revised 26 October 2022; Accepted 1 November 2022; Published 28 December 2022

Academic Editor: Qiang Wu

In order to study the migration characteristics and strata behavior law of mining-induced rocks in fully mechanized caving face of coal mine, taking the actual geological mining of Longwanggou Coal Mine as the background, using computer software (KSPB) to identify the location of key strata. The physical similar material simulation test was used to monitor the movement characteristics of mining-induced rocks by using the internal displacement sensor (IDS) and distributed optical fiber sensor (DOFS). A three-dimensional physical model of 3.6 m × 2.0 m × 2.0 m was built; the internal displacement of rock was measured by IDS. BOTDA distributed optical fiber was used to monitor the dynamic movement and deformation law of coated rock. Finally, the two monitoring results were compared and analyzed. The results show that: (1) the displacement curve of the fractured rock mass in the key strata shows a "stepped" increase; (2) based on the analysis of displacement continuous monitoring results, the strata behavior law of working face is obtained. The first weighting interval of 61601 working face is 90 cm, and the periodic weighting steps are 105 cm, 115 cm, 135 cm, 150 cm, 165 cm, 180 cm, 215 cm, and 240 cm; (3) the average strain of fiber is proposed. The first weighting and periodic weighting laws of the working face are represented by the average strain, which are consistent with the experimental phenomena. The first weighting in the average strain curve shows the first mutation peak, and the periodic weighting shows the periodic mutation peak change of the average strain curve.

1. Introduction

Coal resources account for more than 50% of China's energy consumption [1–5]. For a period of time, coal will still be the main support of China's energy. China's 6 ~ 20 m and above ultrathick coal seam reserves are rich, is the main coal seam of billion tons of large coal base, its resource reserves accounted for 45% ~50% of China's total coal resources [6–9]. China's extrathick coal seams are widely distributed in Shaanxi, Shanxi, Xinjiang, Inner Mongolia, and other regions. With the substantial increase in the degree of mechanization of mines, the current mining of extrathick coal seams is mainly based on one-time full-thickness caving mining [10, 11]. Due to the special mining conditions of extra thick coal seam, the pressure phenomenon in the process of working face advancing is obvious, the stress distribution of stope is complex, and the roof pressure and support working resistance are prominent problems [12–14]. Compared with the general mining height working face, the mining thickness of extrathick coal seam is large, and the migration range of intrusive rock is wide after mining, which leads to more obvious intrusive rock movement. At the same time, disasters such as strong mine pressure, gas outburst, and rock burst occur [15–19]. According to the national statistical data of coal mine accidents from 2010 to 2019, there were 2536 roof accidents, accounting for 44.41% of the total number of coal mine accidents, and 3208 deaths, accounting for 32.28% of the total number of deaths, ranking first in all types of accidents [20]. It can be seen that the prevention and control of roof disasters must

not have any slack. Realizing roof dynamic monitoring and improving support quality are effective means to eliminate roof fall accidents. Therefore, mastering the characteristics of rock breaking and the law of stope pressure behavior is the key technology of coal mine safety production, and also the core problem.

At present, the physical similarity simulation test is mainly used to study the law of erosion rock movement and rock pressure behavior [21, 22]. With the continuous development of test technology, percentage meter, total station, close-range photogrammetry, digital speckle, acoustic emission, and optical fiber sensor are used in physical similarity model test to study the surface displacement, local stress, and deformation law of rock [23–26]. In the two-dimensional plane simulation experiment, total station and close-range photogrammetry technology can directly observe the rock fracture. However, as the uncertainty of the model test itself, the two-dimensional similarity model has a large deviation in reflecting the actual working conditions of the site. More and more scholars use three-dimensional model test to simulate the real ground stress environment for scientific research. In the three-dimensional similar simulation test, the rock fracture is located inside the test model, and the real situation of internal rock fracture cannot be obtained by directly observing the surface. In order to grasp the real activity law of rock strata in the model, Chinese scholars have carried out a series of tests, and used a variety of test methods to obtain the fracture situation and migration law of overlying strata in extrathick coal seam.

Yu et al. [27] studied the rock structure and action mechanism of fully mechanized caving face in extrathick coal seam; Kong et al. [28] used high precision microseismic monitoring technology to study the roof strata movement law of fully mechanized caving face in extrathick coal seam. In order to realize the continuous dynamic monitoring of the internal displacement parameters of the model, it is an effective method to embed displacement sensors in the experimental model, and some applications have been obtained in similar simulation experiment. Chai et al. [29] developed the internal displacement test device, and found that the internal displacement of the model showed a gentle step change; Zhang et al. [30] developed a grating displacement continuous monitoring device and obtained two-band deformation collapse characteristics. However, the displacement sensor can only obtain the displacement of the rock mass in a local range, which cannot realize the multi-scale distributed detection of the internal deformation of the rock mass structure. With the development of the DOFS technology, it provides a new method for rock deformation monitoring [31, 32]. The DOFS and IDS are arranged in the main key layer of the model, and the breaking motion of the key layer in the whole mining stage is monitored in real time and distributed.

Based on the engineering geological background of 61601 fully mechanized caving face in Longwanggou Coal Mine, the internal displacement test system and BOTDA distributed optical fiber are used for three-dimensional physical similarity model test. The characteristics of basic roof breaking, key strata breaking, and caving in real ground stress environment are studied. The first weighting step distance and periodic weighting step distance of three-dimensional model working face are obtained, and the law of mine pressure behavior is expressed. The research is of great significance to grasp the breaking characteristics of overlying strata and the law of strata pressure behavior in extrathick coal seam in this paper.

2. Principle of Optical Fiber Sensing

2.1. Rock Strain Criterion Based on BOTDA. BOTDA sensing technology is based on Brillouin scattering principle, as illustrated in Figure 1. Pulsed light and continuous light are injected at both ends of a complete fiber. When the frequency differences between the two beams are equal to the Brillouin frequency shift of a certain local specific region in the fiber, the stimulated Brillouin amplification effect occurs. Since the Brillouin frequency shift is positively correlated with the ambient temperature and the fiber should be located, in the measurement, the frequency difference of the maximum energy transfer is determined by continuously adjusting the frequency of the two lasers and detecting the power of the receiving end:

$$\begin{aligned} \Delta V_B &= V_{B(\varepsilon)} - V_{B(0)} = C_1 \Delta T + C_2 \Delta \varepsilon, \\ \varepsilon &= [\Delta V_B - C_1 \Delta T]/C_2, \end{aligned} \tag{1}$$

where ΔV_B is Brillouin frequency shift variation; C_1 is the temperature sensitivity coefficient of fiber; $V_{B(\varepsilon)}$ is strain induced Brillouin frequency shift; C_2 is the sensitivity coefficient of fiber to strain; and $V_{B(0)}$ is the initial Brillouin frequency shift to obtain the fiber strain temperature information by detecting the frequency shift change of Brillouin signal and the change of normalized signal power, so as realizing the distributed detection.

2.2. Stress Analysis of Optical Fiber-Rock Layer. In order to monitor the stability of the key stratum under the influence of mining, the horizontal sensing fiber can be arranged in the middle of the key stratum to monitor the deformation process of the rock stratum under the influence of mining in real time.

As shown in Figure 2, under the influence of working face mining, the lower strata are broken down. Under the action of its own gravity, the stress equilibrium state of strata in the horizon where the optical fiber is located is broken, and the optical fiber generates concentrated stress F_m and F_n along the fracture line. After the orthogonal decomposition of F_m and F_n, the horizontal compressive stresses F_{mh} and F_{nh} of the fiber above the goaf are obtained. At this time, in order to maintain the external force balance, the fiber will form the reaction force F_{tm} and F_{tn} in the stable rock above the two sides of the goaf. Therefore, the tensile stress of the fiber above the front and rear sections of the horizontal optical fiber goaf and the "double peak" stress distribution state of the compressive stress of the fiber above the goaf are formed. Stress concentration due to subsidence of fractured rock in optical fiber at both sides of fracture line. This stress is the resultant force of tensile stress, which is caused by the

movement of rock blocks in close contact with optical fiber, and the shear stress on the hinged surface of fractured rock blocks and stable rock strata. So the stress state of the horizontal optical fiber under the influence of mining is distributed in three sections, and the stress concentration on both sides of the fracture line forms the bimodal characteristics of the strain curve. Based on this feature, the "double peak" curve of horizontal optical fiber in the key stratum is used to predict the fracture characteristics of mining-induced rock and predict the stope weighting.

2.3. Average Strain Variation of Optical Fiber. Strain value measured by distributed optical fiber is the reflection of external deformation of sensing fiber. When the sensing fiber is embedded in the rock, different rock deformation and collapse state will cause different frequency shift values. If the rock stratum produces small deformation, the frequency shift value is small, and the strain value is also small. On the contrary, the rock strata have large deformation or even break and fall, the strain value will also increase. According to this theory, the strain value measured by distributed optical fiber can be used to determine the breaking law of overlying strata (or the law of strata behavior). The concept of average strain variation of optical fiber is defined as the average strain variation of optical fiber embedded in rock during rock deformation. The calculation method is:

$$D_x = \frac{\sum_{i=1}^{n_f} \varepsilon}{n_f}, \tag{2}$$

Where D_x represents the average strain of optical fiber test when the excavation distance of working face is x; n_f is the number of test points on the optical fiber, which is determined by the sampling interval of the test instrument. It is 5 cm in this test. For example, the test length of the optical fiber in the model test is 360 cm, and the number of test points n_f is 72. ε is the strain value for each test point.

The physical meaning of average strain is that it represents the deformation of rock strata. The greater the average strain, the higher the degree of deformation and failure of rock strata, that is, the breaking movement of rock strata is violent. Therefore, when the average strain has a large 'step' change, it means that the strata have a large fracture movement. In other words, when the first weighting or periodic weighting of overlying strata occurs, the average strain will inevitably have a large step.

3. Three-Dimensional Physical Similarity Simulation Experiment

3.1. Engineering Geology. The designed production capacity of Longwanggou Coal Mine is 10.0 Mt/a, and the production mode of "one well and one side" is adopted during transfer. The terrain is generally high in the west and low in the east. The surface is scoured by rain, and the gully is developed. There is no spring dew point, and most of them are ditches in the rainy season. There is no perennial water on the ground and no old kiln area. The first mining face is 61601 working face in 61 panel area, thickness of coal seam between 18.8 ~ 28.8 m and the working face adopts comprehensive mechanized top coal caving mining technology. Compared with the conventional layered mining, the mining height of thick coal seam increases, the height of caving zone increases, the periodic caving distance is larger, and the impact is greater.

The test prototype is 61601 fully mechanized caving face in Longwanggou Coal Mine, and the buried depth is 412 m. The strike length is 615 m and the dip length is 254.6 m, as shown in Figure 3. The working face mining coal seam is No. 6 coal seam thickness between 18.8 ~ 28.8 m, the average thickness is 23.83 m, dip angle is 0 ~ 5°, the average is 2.75°, is stable coal seam.

3.2. 3D Physical Model Construction. In order to make the similar model accurately reflect the objective law of engineering practice, this experiment will simulate all the overlying strata in 61601 working face of the coal mine. Combined with the geological conditions and similar simulation test conditions in the study area, the model frame with the size of 3600 (length) ×2000 (width) ×2200 (height) mm was finally selected. The basic parameters of the three-dimensional physical similarity model are shown in Table 1. The coal seam thickness of the model is 100 mm, the total thickness of the upper strata is 1870 mm, the length of the working face 1 is 1200 mm, the length of the working face 2 is 600 mm, and the advancing length is 2600 mm. There are 500 mm boundary coal pillars at the front and rear boundaries, and 200 mm boundary coal pillars at the left boundary of the model, as shown in Figure 4. Due to the large volume of three-dimensional model test, the ordinary coal seam excavation method is not applicable, so the test uses the form of strip pipe to simulate coal seam excavation. The rectangular galvanized square pipe is laid above the 60 mm bottom plate, the section size of the square pipe is 100 × 50 mm, which is used to simulate the thickness of the coal seam and the excavation footage of the coal seam, that is, the thickness of the coal seam is 100 mm, and 50 mm each excavation.

The physical similarity model selects gypsum and white powder as the transition material, and river sand as the aggregate. Mixing different proportions of similar materials to simulate different strata, the rock parameters as shown in Table 2.

According to the key stratum theory of strata control, the key stratum and its position in Longwanggou Coal Mine are discriminated by using the key stratum discrimination software (KSPB) [33], and the position of each key stratum is calculated as shown in the table. In order to accurately describe the change characteristics of each key stratum, it is numbered from bottom to top, namely KS1 ~ KS7. The key stratum near the working face is KS1, and the key stratum near the surface is KS7, as shown in Table 2. In the experiment, the height of the rock layer and the position on the model are arranged according to the position of the key stratum.

3.3. Monitoring System Layout. In order to study the characteristics of rock movement and strata behavior in advancing

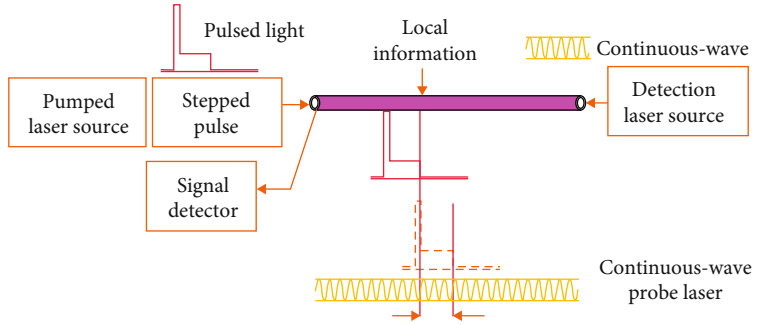

Figure 1: Working principle of BOTDA.

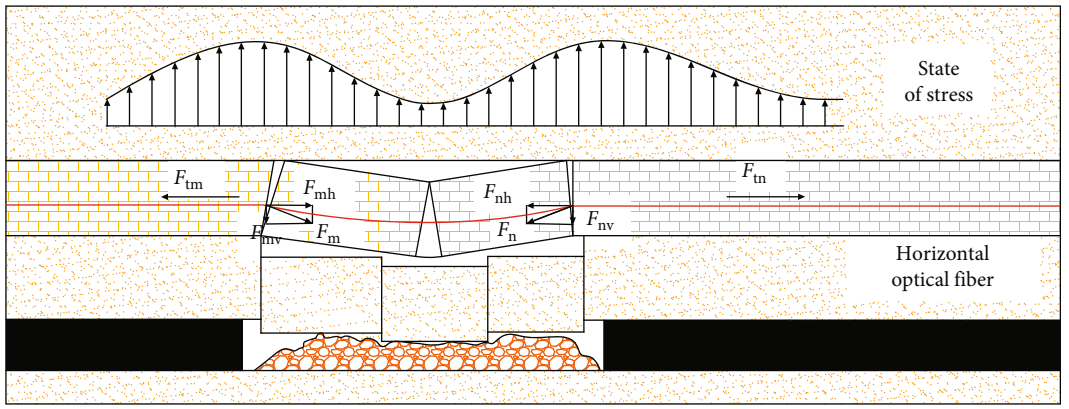

Figure 2: Fiber stress distribution.

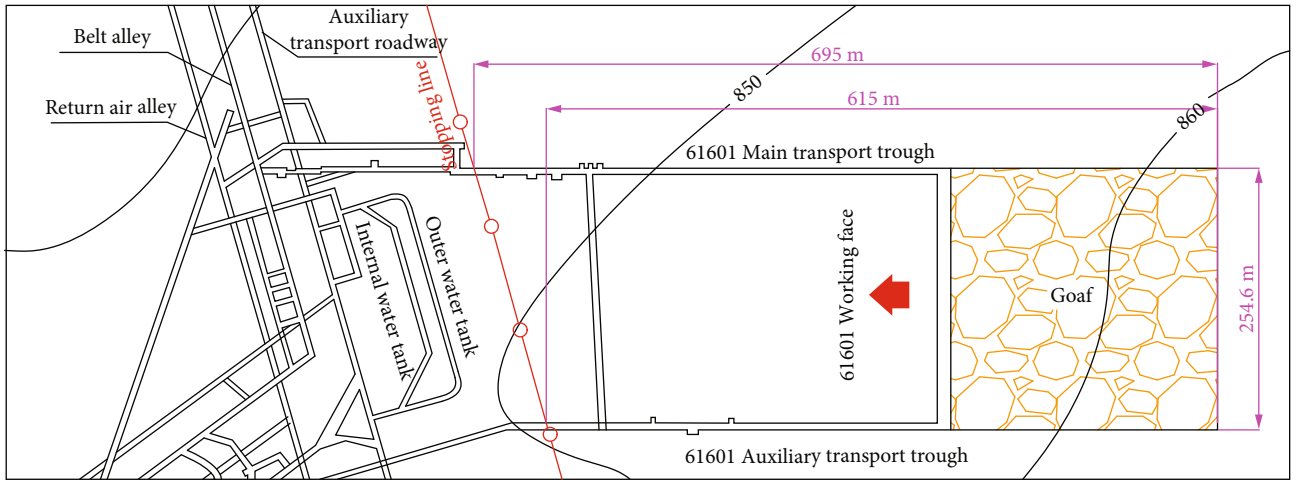

Figure 3: 61601 working face layout position.

process of working face, the internal displacement continuous monitoring device and distributed optical fiber testing device are used to accurately and real-time monitor the fracture of key strata.

3.3.1. Internal Displacement Test Device. Four sets of displacement measuring devices are arranged in the rock of the model working face, and two displacement measuring surfaces are arranged above the two working faces. The first layer displacement measuring surface of working face 1 is located in KS3 coarse sandstone, and the measuring point numbers are 111 # and 121 #, respectively. The displacement measuring surface of the second layer is located in KS7 coarse sandstone, and the number of measuring points is 112 # and 122 #, respectively. Similarly, the four displacement measuring points of working face 2 are 211 #, 221 #,

Table 1: Basic parameter table of 3D physical similarity model.

Item	Parameter	Item	Parameter
Length	360 cm	Width	200 cm
Height	200 cm	Excavation steps	54 steps
Thickness of coal seam	10 cm	Single excavation distance	5 cm
Geometric similarity ratio	1 : 200	Excavation time interval	0.5 h
Similarity ratio of bulk density	1.56 : 1	Stress similarity ratio	380 : 1

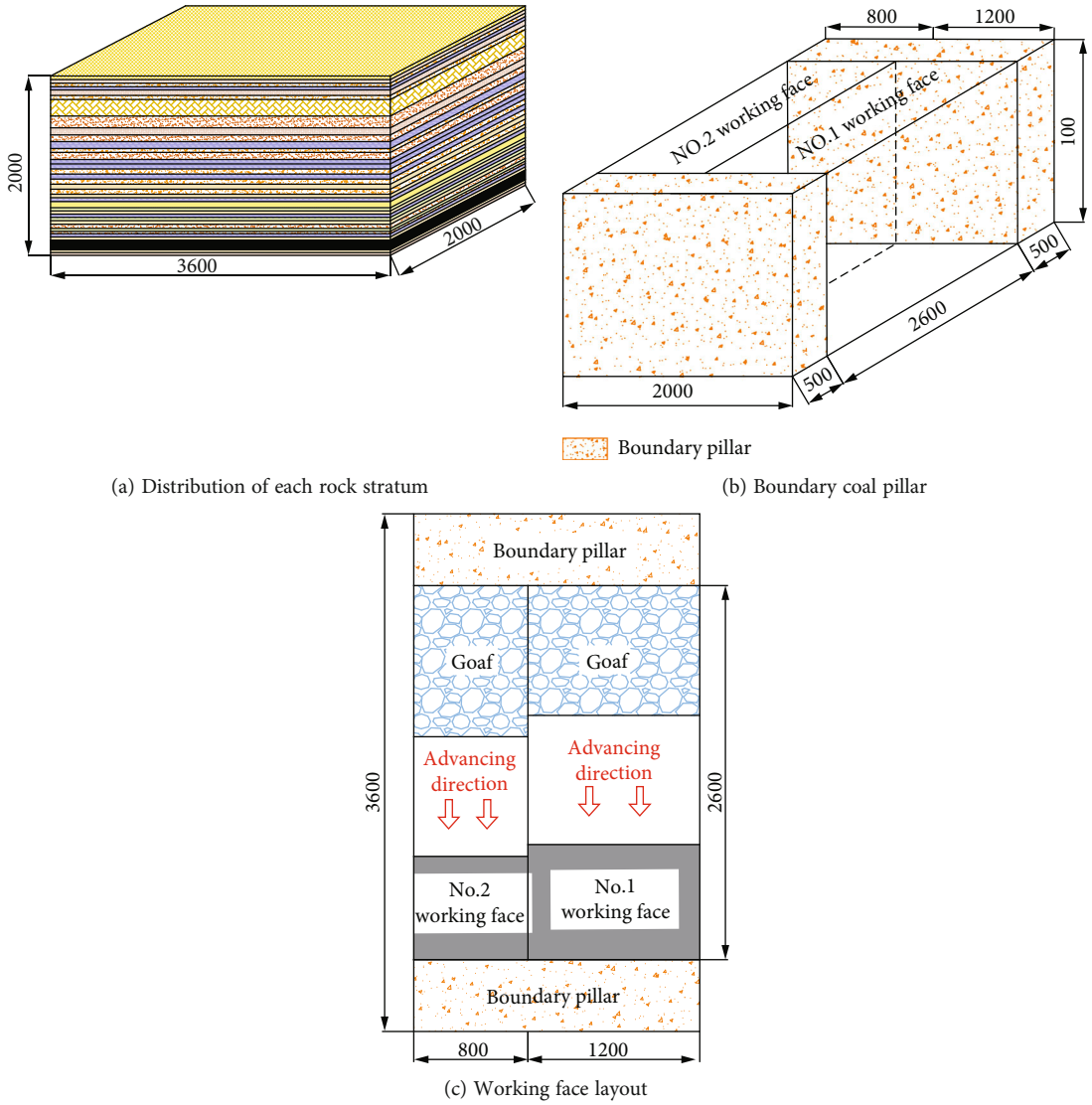

(a) Distribution of each rock stratum

(b) Boundary coal pillar

(c) Working face layout

Figure 4: 3D similar material simulation model.

212 #, and 222 # in turn. The layout of measuring tubes and displacement points in the model paving process is shown in Figure 5.

3.3.2. Optical Fiber Testing System. In order to realize the distributed detection of mining rock deformation characteristics, a distributed optical fiber test system is arranged in the model. Distributed optical fiber detection system is formed from the direction and height of coal seam (rock), as shown in Figure 6. The distributed sensing fibers in the model can be divided into two groups. Namely, horizontal optical fibers are arranged along the strike direction of the working face, numbered FH11, FH12, FH21, and FH22. Vertical fibers are arranged along the height direction of the model, numbered as FV11, FV12, FV21, and FV22.

The installation of DOFS is embedded, that is, the installation of optical fiber system is completed in the process of model paving. When the model is paved to the design layer,

Table 2: Parameters of each rock stratum.

Serial number	Lithology	Mean thickness of layers/mm	Density/ kg·m^{-3}	Remark	Serial number	Lithology	Mean thickness of layers/mm	Density/ kg·m^{-3}	Remark
31	Loess	115	1790		15	Mudstone	10	2330	
30	Fine sandstone	110	2650		14	Grit stone	50	2560	
29	Grit stone	95	2560		13	Sandy mudstone	25	2600	
28	Sandy mudstone	10	2600		12	Grit stone	100	2560	
27	Fine sandstone	210	2650		11	Sandy mudstone	10	2600	
26	Fine sandstone	175	2560	KS7	10	Grit stone	65	2560	KS3
25	Fine sandstone	125	2650	KS6	9	Mudstone	15	2330	
24	Sandy mudstone	75	2600		8	Grit stone	45	2560	KS2
23	Fine sandstone	70	2650	KS5	7	Coal	5	1400	
22	Mudstone	45	2330		6	Mudstone	25	2330	
21	Sandy mudstone	70	2600		5	Grit stone	25	2560	KS1
20	Grit stone	75	2560	KS4	4	Sandy mudstone	20	2600	
19	Sandy mudstone	70	2600		3	Coal	10	1400	
18	Grit stone	65	2560		2	Grit stone	25	2560	
17	Mudstone	45	2330		1	Mudstone	15	2330	
16	Grit stone	70	2560		0	No. 6 coal seam	100	1400	

the optical fiber is installed inside the model rock, and the optical fiber is fixed once every 200 mm by the optical fiber fixed caliper to ensure that it is buried in the rock layer. At the same time, the top and bottom winding fixer of the vertical fiber is designed and installed, which is used to install the fixed vertical fiber and has a given prestress. In order to accurately obtain the deformation information of internal rock strata, NBX-6055 sonar was used in this experiment. The instrument parameters were selected as follows: 5 cm spatial resolution, 2×10^{16} averaging times, and 5 cm sampling interval. 2 mm single-mode fiber is selected, which can meet the requirements of large deformation strength such as collapse and fracture of overburden rock, and almost does not affect the movement of overburden rock.

4. Result and Discussion

4.1. Fracture Characteristics of Key Strata. The working face is excavated 5 cm every 30 min, and the fracture characteristics and variation law of each key stratum in the process of coal seam mining are obtained, as shown in Figure 7. Working face 1 advancing to 35 cm, the key stratum KS1 first broken, caving length of 21 cm, KS1 fracture caused the lower strata synchronous broken caving to goaf, as shown in Figure 7(a). When the working face 1 advances to 60 cm, the key stratum KS2 first breaks and the collapse length reaches 36 cm, as shown in Figure 7(b). The KS2 fracture causes the synchronous fracture instability of the upper strata and the rotation movement. When the KS2 fracture occurs, the KS3 structure maintains stability and reduces the strength of the KS2 fracture to a certain extent. As the large thickness of the coal seam, a larger mining space will be formed after the coal seam is mined, the scope of the overlying rock will also increase, and the immediate roof strata collapse in time with the mining of the working face.

As the working face 1 continues to advance to 90 cm, the goaf area behind the working face increases, and the basic roof (KS3) is broken for the first time. After the key layer KS3 is broken, the masonry beam structure is formed, and the caving length is 65 cm. The working face produces the first weighting, as shown in Figure 7(c). With the continuous mining of the working face to 105 cm, the basic roof (KS3) is periodically broken. The span of the broken rock block is 80 cm and the collapse height is 55 cm, forming a cantilever beam and masonry beam combination structure. The rock breaking span and strength are increased, as shown in

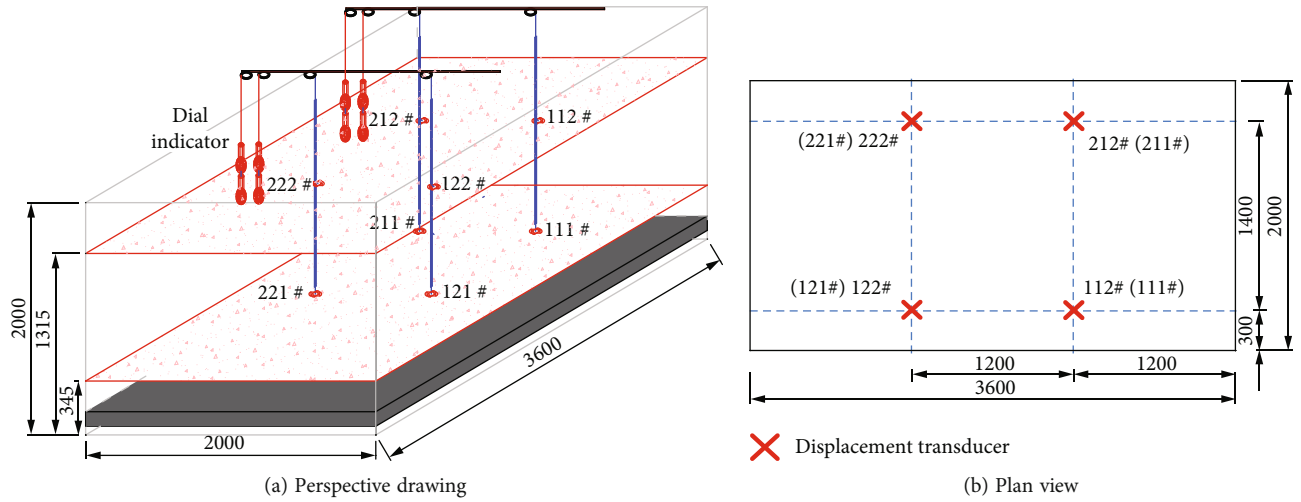

(a) Perspective drawing (b) Plan view

Figure 5: Schematic layout of displacement measuring points.

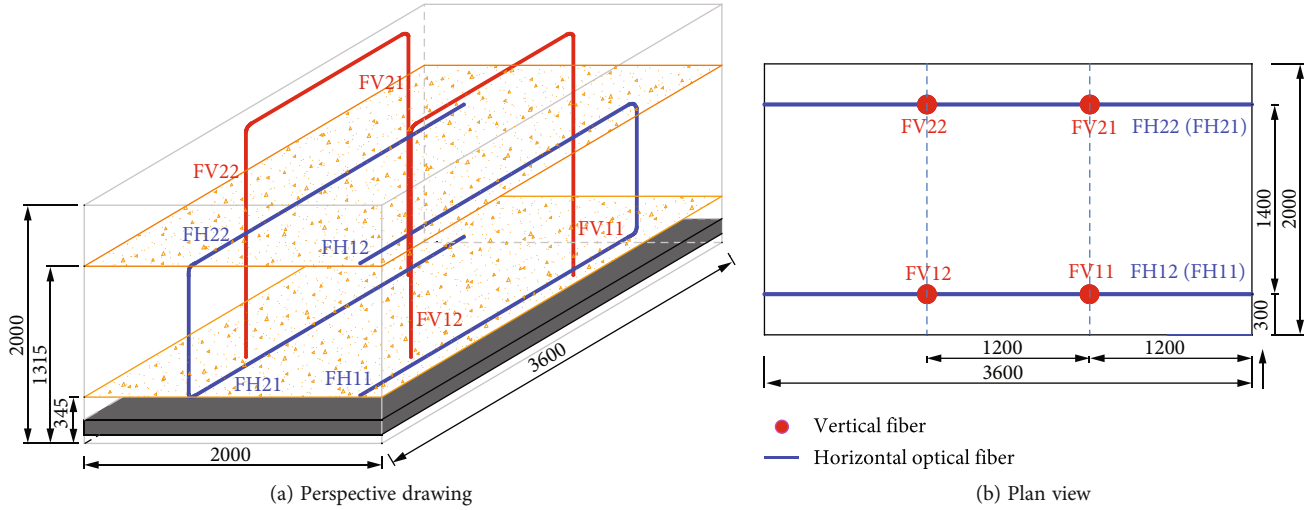

(a) Perspective drawing (b) Plan view

Figure 6: The layout of optical fiber testing system.

Figure 7(d). The thickness of key stratum KS3 is 6.5 cm. Because of its large thickness and large span of broken unstable rock mass, the energy release intensity after breaking is high, resulting in the synchronous breaking rotation movement of underlying strata and acting on the support of working face, resulting in the increase of working resistance of support and the strong periodic weighting of working face. The near-field cantilever beam structure instability acts on the composite cantilever beam structure, and the joint rotation acts on the working face. The periodic breaking instability of the near-field cantilever beam and the masonry beam structure causes the "large and small periodic" weighting characteristics of the working face.

As the working face continues to advance to 135 cm, the median rock caving width is 68 cm, and the rotary subsidence is 7 cm. The instability and fracture of the median rock structure, together with the instability and movement of the low structural rock, causes the strong mine pressure phenomenon of the working face, as shown in Figure 7(e).

As shown in Figure 7(f), when the working face is mined to 165 cm, the KS4 first breaks, the span of the broken rock block reaches 63 cm, and the breaking rotary subsidence reaches 3.7 cm. The thickness of key stratum KS4 is 7.5 cm, and the thickness of rock stratum is large and the caving length is long. The high energy is released after breaking, resulting in the synchronous breaking movement of underlying rock stratum and acting on the working face. The cantilever structure of KS1 and KS2 has a certain degree of protection on the working face, so the impact on the working face is slightly lower than that of KS3.

As the working face continues to be mined to 200 cm, the key layer KS5 is broken for the first time. The length of broken rock reaches 70 cm, and the thickness of KS5 is 7 cm, as shown in Figure 7(g). KS5 fracture releases large energy and high strength, resulting in synchronous fracture of key strata of KS1 ~ KS4, and acts on the working face, resulting in strata behavior. As the working face continues to advance to240 cm, high key layer KS6 breaks, breaking rock length of 80 cm, KS6 thickness of 12.5 cm, as shown in Figure 8(h). As the working face continues to advance to 240 cm, high key layer KS6 breaks, breaking rock length of 80 cm, the thickness of KS6 is 12.5 cm, as shown in Figure 7(h). Because the thickness of

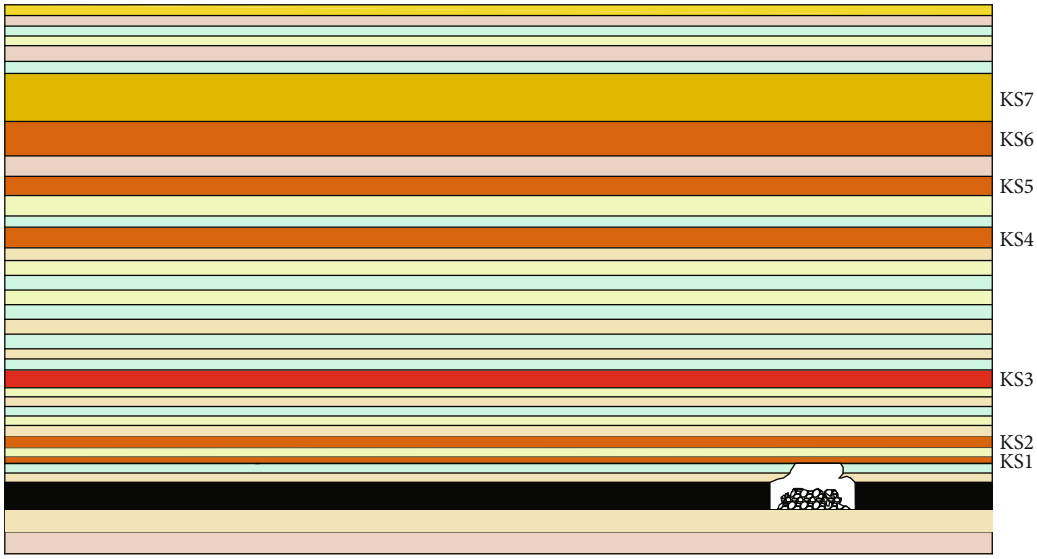

(a) Initial breaking of key stratum KS1

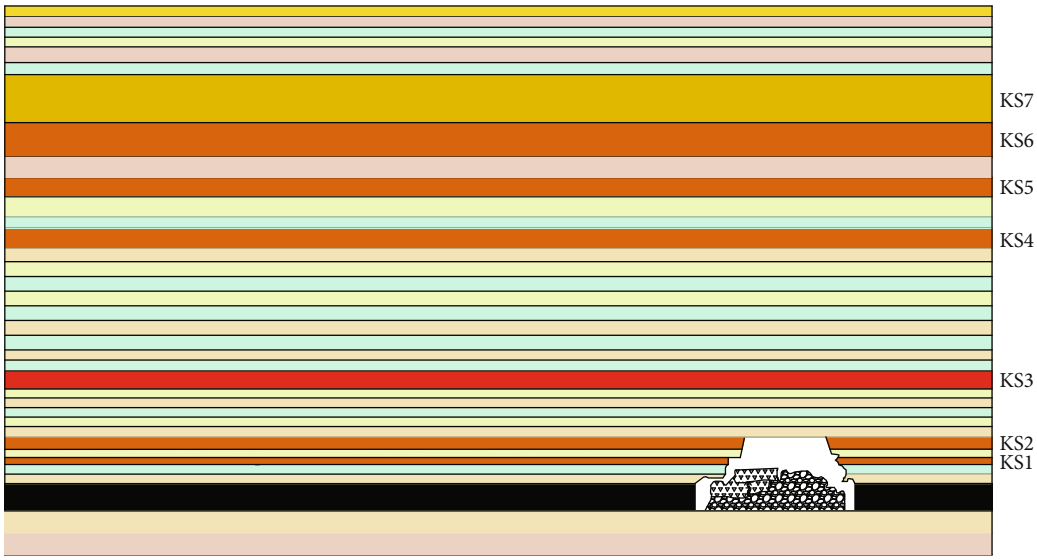

(b) Initial breaking of key stratum KS2

Figure 7: Continued.

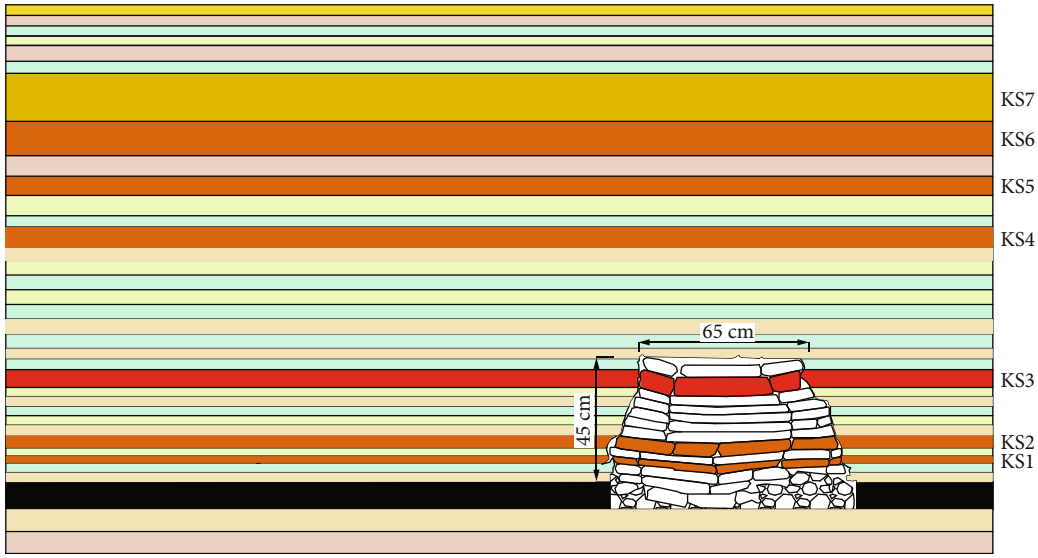

(c) Initial weighting of working face

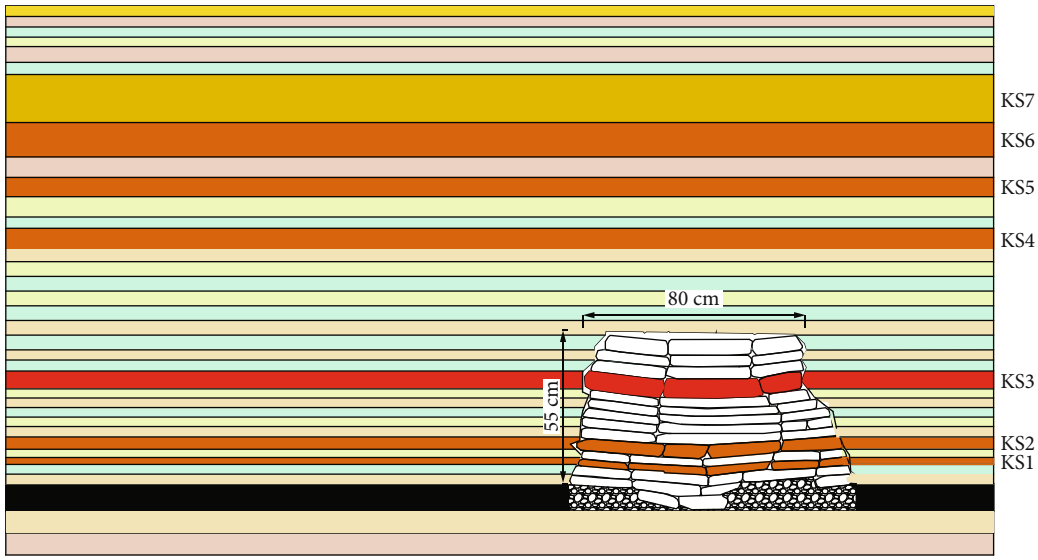

(d) First periodic weighting

Figure 7: Continued.

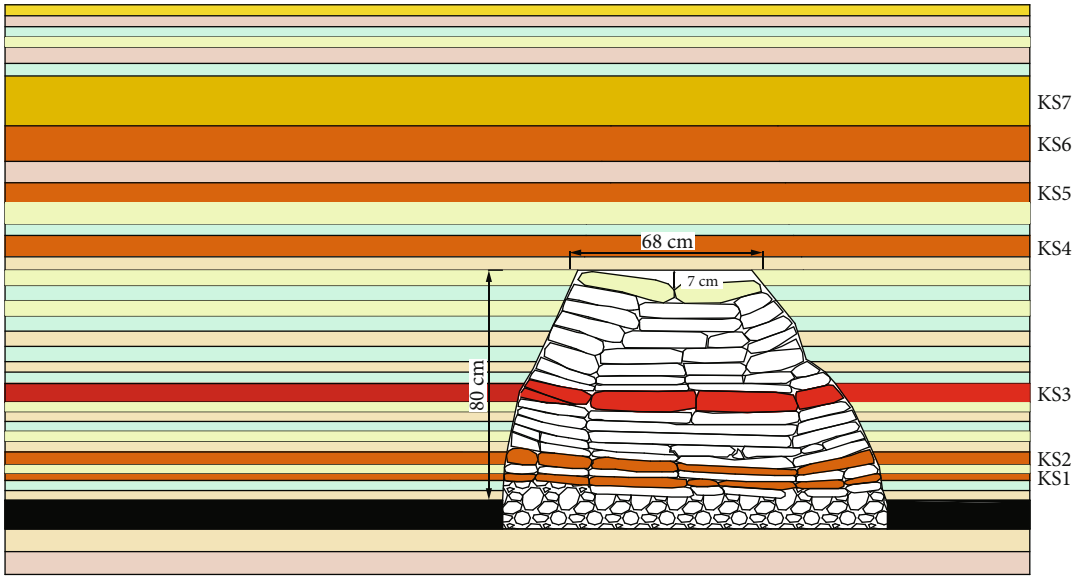

(e) Fourth periodic weighting

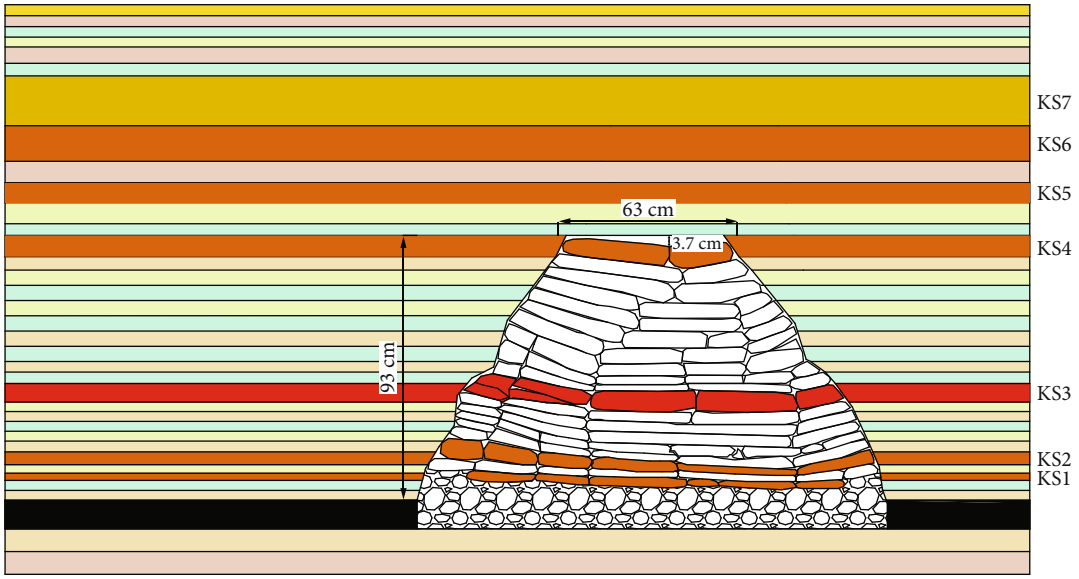

(f) KS4 initial break

Figure 7: Continued.

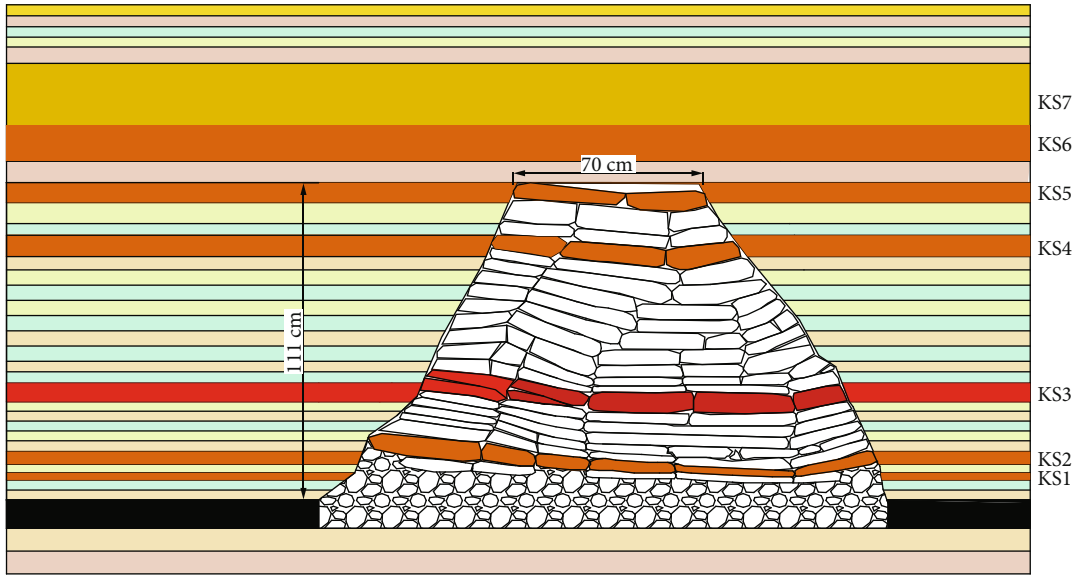

(g) KS5 initial break

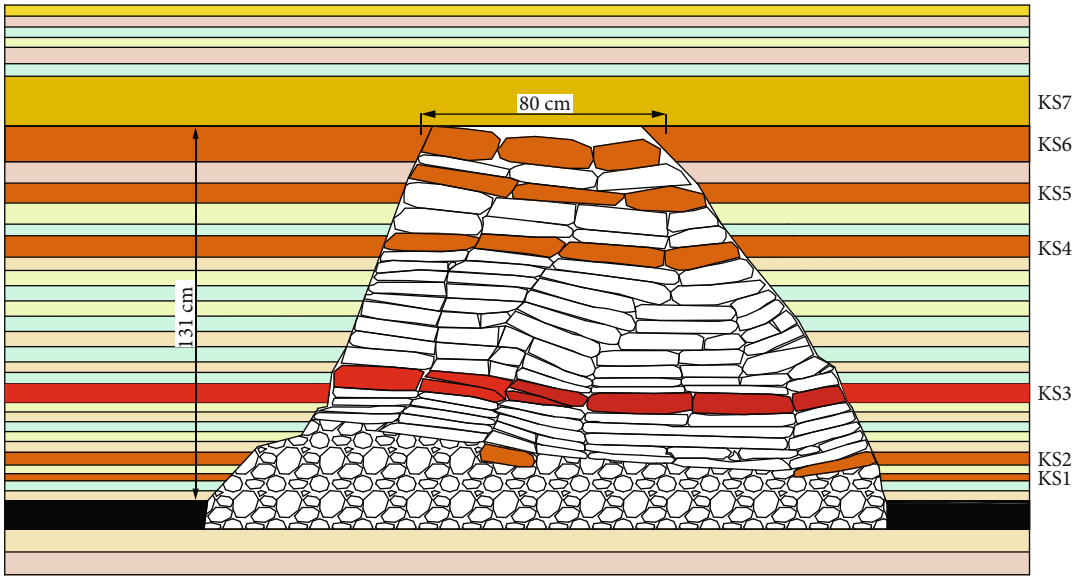

(h) KS6 initial break

Figure 7

KS6 is larger and the energy released by fracture is high, the lower rock strata are unstable and rotated after fracture, resulting in large displacement, and the impact on the working face is larger than that of KS5.

Through the above analysis of rock structure fracture evolution, it can be seen that the fracture length of the low key layer is greater than that of the high key layer, and the periodic weighting times are more frequent, which will produce obvious weighting phenomenon. In the near-field rock structure, the low key stratum (KS3) is unstable and broken to form a "cantilever beam" structure, and its periodic fracture produces small periodic weighting. When the fracture instability of the intermediate rock structure (KS3 ~ KS5) moves with the low structural rock strata, strong strata behavior will occur. Affected by the gradual crushing movement of rock strata, the structure of high rock strata is relatively stable, and the span of broken rock strata is large. When it is broken and unstable, it will move synchronously with the near-field rock structure below it, resulting in strong weighting. Therefore, the breaking instability of the high key strata (KS6 ~ KS7) is the main factor causing the strong strata behavior of the working face.

4.2. Deformation and Fracture Characteristics of Key Layer Based on Continuous Displacement Monitoring. The key stratum KS3 is a key stratum near the coal seam, which forms a hinge structure. Its mechanical response characteristics and the fracture migration law of key blocks directly

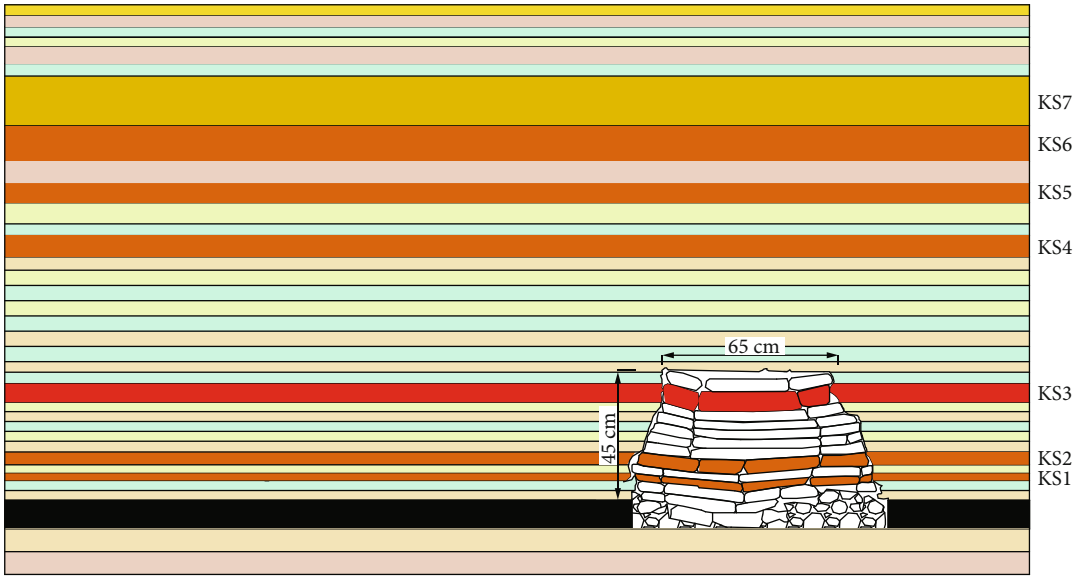

(a) The first weighting step

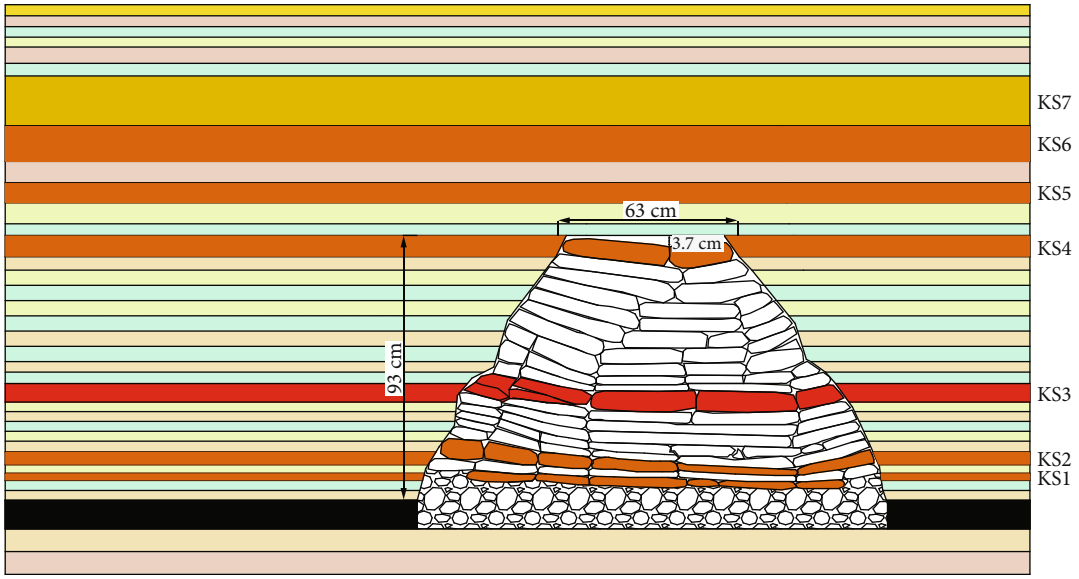

(b) Periodic weighting

Figure 8: Continued.

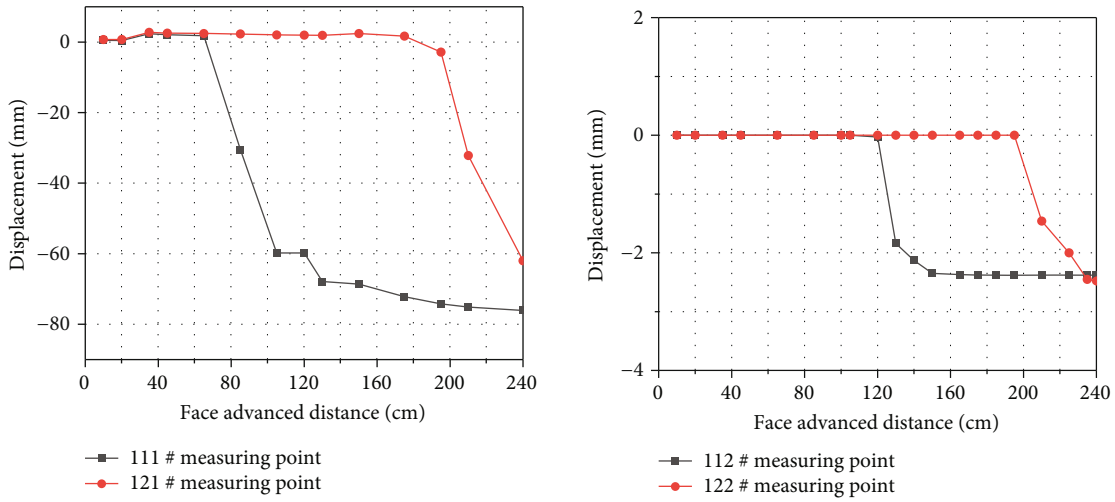

(c) Displacement curve of key layer KS3 measuring point

(d) Displacement curve of KS7 measuring point in main key layer

Figure 8: Detection results of internal displacement test system.

affect the change of collapse space. The test results of the monitoring points are shown in Figure 8(c). The working face is promoted by the open-off cut, and the displacement of each monitoring point increases periodically. The displacement curve shows a "step" change, and the maximum displacement reaches 76 mm. When the working face advances to 0 ~ 40 cm, each monitoring point is less affected by mining in front of the work, and the displacement of the monitoring point is almost 0 mm. When the advancing distance of working face is 50~70 cm, the displacement of 111 monitoring points increases slightly, which indicates that the bending deformation of key stratum KS3 occurs under the action of overlying strata and self-weight. When the working face advances to 90 cm, the displacement of 111 monitoring points suddenly increases to 31 mm, indicating that the key layer KS3 first breaks, so the first weighting step of working face 1 is about 90 cm, which is also consistent with the experimental phenomenon. With the working face advancing to 105 cm, the displacement of 111 # monitoring point increased again, indicating that the broken rock near the monitoring point had violent movement, and the first periodic weighting occurred in the model working face 1. The working face continued to advance from 165 cm, and the displacement of monitoring point 111 # continued to increase, indicating that the goaf was gradually compacted under the gravity of the broken rock block.

When the advancing distance of the working face is 90–195 cm, the displacement of the 111 # monitoring point increases gradually with the increase of the advancing distance, but the displacement of the 121 # monitoring point is almost 0, indicating that the collapse range of the key layer KS3 does not reach the monitoring area of the 121 # monitoring point. When the working face advanced to 195 cm, the displacement of 121 # monitoring point increased to 2.9 mm, indicating that the bending deformation of the key layer KS3 caused the displacement of 121 # monitoring point. When the working face advances to 200 cm, the displacement of 121 # monitoring point suddenly increases to 38 mm. It is speculated that the KS3 of the key layer is broken periodically, and the displacement of 111 # measuring point also occurred but the displacement is small. The high key layer is broken and collapsed, and the broken rock in the goaf is further compacted, resulting in the displacement of 111 # measuring point increased. Similarly, when the working face is advanced to 240 cm, the displacement of 121 # monitoring point increases sharply to 60 mm, and the displacement of 111 # monitoring point increases slightly. It is speculated that the key layer KS3 is broken periodically again, and the movement of rock is more intense.

In order to obtain the mining response law of the main key layer KS7, the displacement data of 112 # and 122 # monitoring points are selected on the basis of the second layer displacement surface. The test results of the monitoring points are shown in Figure 8(d). Compared with the subsidence displacement of the key stratum KS3 fracture rock mass, the displacement of the main key stratum fracture rock mass is significantly reduced. The maximum subsidence of the monitoring point is 2.5 mm, and the displacement of the fracture rock mass changes slowly. The above analysis shows that when the working face advances to about 90 cm, the key layer KS3 first breaks. At this point, the displacement of 112 # monitoring point is about 1.9 mm, indicating that the bending deformation of the main key layer did not break. As the working face advances to 215 cm, the displacement of 112 # measuring point does not change significantly. The displacement of 122 # measuring point increases to 1.5 mm, and the displacement is very small, indicating that the influence of mining on the main key layer is small.

In summary, when the key stratum is broken, the displacement of each monitoring point increases sharply, and the subsidence curve of the key stratum KS3 broken rock mass increases step by step. Compared with the experimental phenomenon, it shows that the internal displacement monitoring results can reflect the working face pressure.

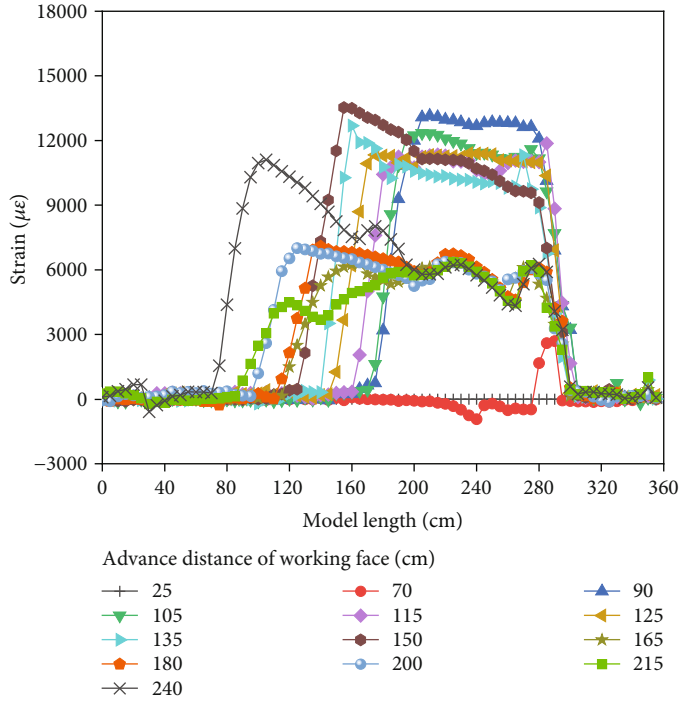

(a) Strain test curve of horizontal fiber FH11

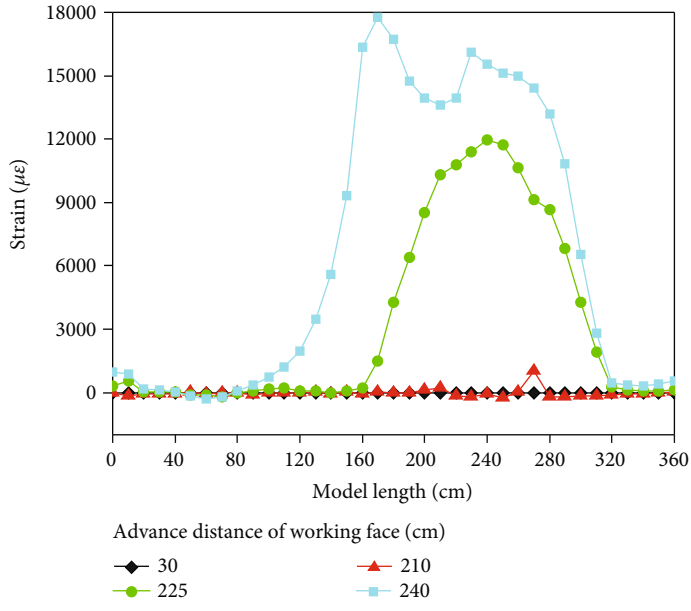

(b) Strain test curve of horizontal fiber FH12

Figure 9: Test results of horizontal fiber.

4.3. Migration Characteristics of Stope Rock Based on Optical Fiber Monitoring

4.3.1. Horizontal Fiber Response Characteristics of Key Layer Deformation. Figure 9(a) is the strain curve of the horizontal optical fiber FH11 with the advancing of the working face. The transverse coordinate is the model length, and the ordinate is the strain value of the sensing fiber. It can be seen from the figure that the strain variation range of the horizontal fiber is much larger than that of the excavation range of the working face. There are two reasons for this phenomenon: firstly, the existence form and distribution state of horizontal optical fiber in three-dimensional model test are different from those in two-dimensional model. In the three-dimensional model, the optical fiber is affected by the strike and inclination of the coal seam in the horizontal direction. Even if the lateral stress has little effect, it will still lead to the strain of the optical fiber. Second, the buried horizon of FH11 is located at the height of 345 mm, that is, 145 mm above the coal seam, just in the key layer KS3.

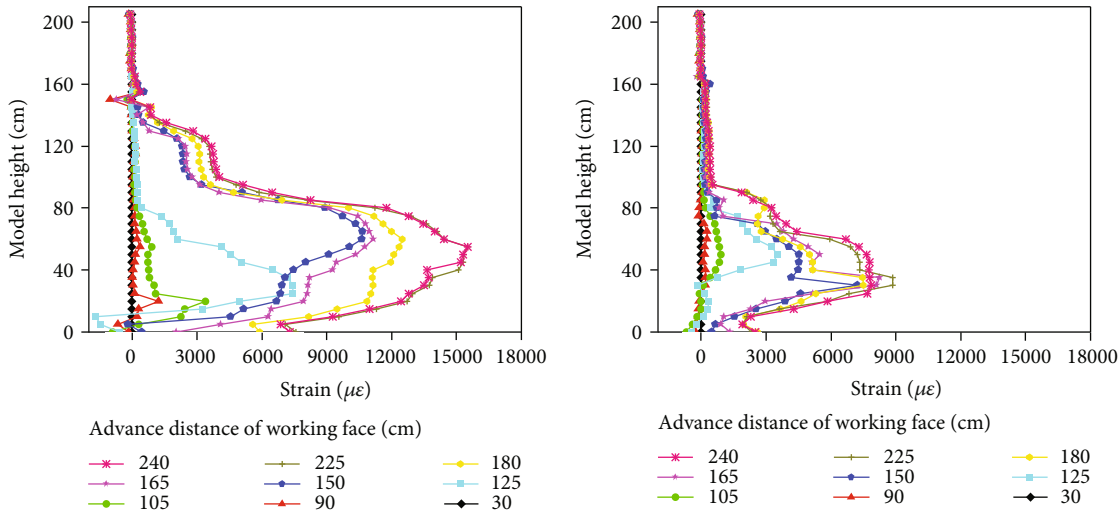

(a) Strain test curve of vertical fiber FV11

(b) Strain test curve of vertical fiber FV12

Figure 10: Test results of vertical optical fiber.

Generally speaking, under the influence of mining (or when there is free space below the rock stratum), interlayer separation will occur between the hard rock stratum and the soft rock stratum. From the test phenomenon, it can also be found that the rock stratum at 345 mm has collapsed, and the key layer KS3 is in the hinged structure.

According to the fracture characteristics of the key layer in section 4.1, when the working face advanced to 90 cm, the first weighting occurs. The KS3 is broken and the main roof is collapsed. From Figure 9(a), it is found that the fiber exhibits bimodal characteristics, which conforms to the stress distribution of the fiber and the peak strain curve reaches 13155 $\mu\varepsilon$. In view of the above analysis, the strain curve of 90–240 cm working face is taken. In this range, the two ends of the strain curve are raised, showing obvious bimodal characteristics, and the peak on the right side is obvious. The peak on the left side continues to move to the left with the advancement of the working face, but the concave in the middle of the curve is not obvious, indicating that the rock strata between the fracture lines more. Therefore, it can be determined that in the range of 0 ~ 345 mm model height, the rock formed two continuous upward development fracture lines, and the mining effect of the working face is obvious.

Figure 9(b) shows the strain variation curve of horizontal fiber FH12 with the advancing of working face. FH12 is located at the height of 1400 mm, which is located in the middle of the main key layer (KS7), and its strain distribution is the manifestation of the deformation movement law of the main key layer. According to the data analysis in the diagram, the internal deformation characteristics of the key layer of the horizontal fiber FH12 are obtained:

(1) When the working face is excavated 0 ~ 300 mm, the advancing distance of the working face is short, and the test strain curve has no obvious change, indicating that the test strata are not affected by mining

(2) When the working face is excavated 300~1150 mm, the test strain value is positive, the strain curve forms a single peak, and reaches the maximum bending state at the 1200 mm length of the model, which indicates that the bending of the main key layer produces cracks but does not break, and only bends downward in the range of 0 ~ 2000 mm of the working face. At the distance to the left of the model length of 2000 mm, the strain test curve tends to be flat, indicating that the optical fiber test strata within this distance have not been affected by mining

(3) When the working face is excavated from 1150 mm to 2400 mm, the two ends of the strain curve in this range are raised, showing obvious bimodal characteristics, and the peak on the right side is obvious. The peak on the right side continuously moves to the right with the advancement of the working face. When the strain curve excavated at the working face of 1150~2400 mm in the figure, a serrated curve change appeared in the middle of the double peaks, and some serrated spacing was close, which was also the manifestation of multiple longitudinal cracks in the main key layer in the experiment

4.3.2. Vertical Fiber Response Characteristics of Key Layer Deformation. Two vertical optical fiber sensors (FV) embedded in the model are arranged along the advancing direction of the working face, which are 700 mm and 1900 mm ahead of the open cut. As shown in Figure 10(a), according to the strain test curve of vertical fiber FV11, the breaking motion law of each key layer in vertical direction is obtained:

(1) When the working face is excavated 0 ~ 300 mm, the working face is excavated at the position of the optical fiber, and there is a certain distance from the optical fiber. The strain test curve has no obvious change, indicating that the test area is not affected by mining

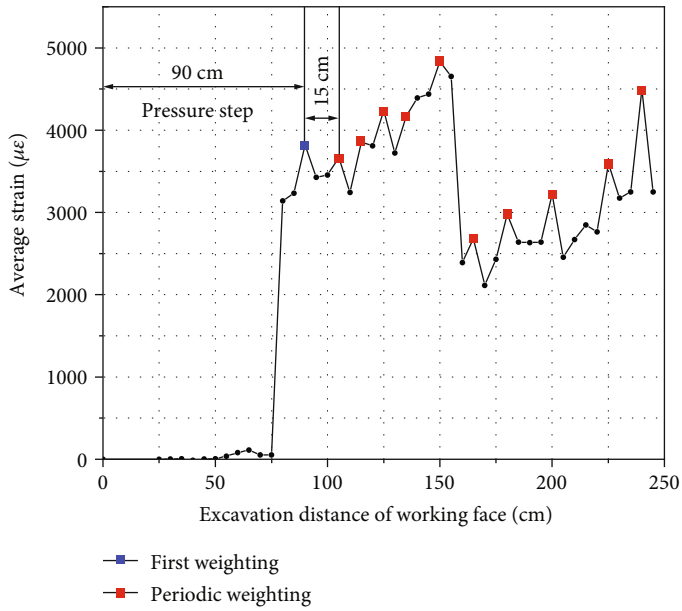

Figure 11: Strain average variation curve of fiber.

(2) When the working face is excavated to 900 mm, the working face passes through the optical fiber buried area, and the test strain value is positive. The strain curve forms a unimodal shape, indicating that the deformation and movement of the optical fiber test rock strata occur. Different deformations are presented at different heights, so that the fiber strain varies at different heights. Overall, with the increase of model height, the variation of strain value decreases gradually

(3) When the working face is excavated 900~2400 mm, the working face pushes through and away from the rock layer where the optical fiber is located, the test strain curve changes: in the range of 0 ~ 150 mm of model height, the strain curve shows a negative change, indicating that the tested rock strata are in the state of compressive stress in this range, which is the characterization of the recompaction of rock strata in goaf. However, in the model height range of 150~1450 mm, the strain curve shows new characteristics: the strain value is positive, the strain curve is unimodal, and the strain peak is near the model height of 650 mm, indicating that the rock strata in this height range are in tensile stress state, and the rock strata are still moving downward. In the range of model height from 1450 mm to 1600 mm, the strain value turns to be negative again, and the strain curve forms a reverse negative unimodal shape, indicating that this section of rock is in the state of compressive stress

As shown in Figure 11, according to the FV12 strain test curve of vertical optical fiber, the fracture and collapse of each key layer in the vertical direction are obtained: when the working face is excavated 0 ~ 900 mm, the working face is far away from the rock where the optical fiber is located, and the strain test curve has no obvious change, indicating that the optical fiber test rock is not disturbed. When the working face is excavated from 900 mm to 1050 mm, the strain test curve begins to change slowly, indicating that the rock strata in the optical fiber test are deformed and moved, showing different deformation sizes in different heights, so that the optical fiber strain varies in different heights.

When the working face is excavated 1050~2400 mm, the working face advances towards the optical fiber buried area, and the strain test curve shows significant changes: in the range of model height from 0 mm to 950 mm, the strain curve showed a positive change and a single peak. The peak strain is located near the model height of 350 mm, indicating that the rock layer within this height range is in the tensile stress state, and the rock layer moves downward, corresponding to the caving zone height of 350 mm. When the model height is above 950 mm, with the increase of model height, the variation of strain value gradually decreases and tends to be 0, and the strain curve becomes flat, indicating that this section of rock is not affected by mining.

4.4. Analysis of Mine Pressure Law Based on Average Strain. Based on the monitoring results of horizontal fiber, the strain average degree of fiber test in this model test is calculated according to Formula (2). As shown in Figure 11, the abscissa represents the advancing distance of the working face, and the ordinate represents the average strain of the optical fiber test. It can be found from the strain average curve that the curve is serrated distribution. Each peak in the curve sawtooth distribution indicates that a large deformation occurs suddenly in the key layer KS3 at the excavation distance, resulting in a significant increase in the optical fiber test strain in the model. Considering the fracture movement process of the upper strata, the initial fracture and periodic fracture of the old roof will lead to large deformation and movement of the strata. Therefore, it can

be considered that the mutation of the strain average degree curve is the manifestation of the strata pressure law of the mining-induced erosion rock working face, specifically.

As shown in Figure 11, there are 11 strain average sawtooth peaks in the figure, the first peak appears when the working face advances to 90 cm (blue point in the figure), then 105 cm, 115 cm, 125 cm, 135 cm, 150 cm, 165 cm, 180 cm, 200 cm, 215 cm, and 240 cm appear cyclic peak (red point in the figure), which is consistent with the IDS test results. Therefore, the working face weighting can be interpreted from the fiber strain average curve, such as the first weighting step distance is 90 cm; the first periodic weighting step distance is 105 cm. In addition, the strength of the strata behavior can be determined according to the peak value of the strain average sawtooth in the figure. For example, when the working face is excavated to 165 cm, the mutation peak of strain average degree is small, indicating that the rock pressure behavior is relatively weak. The reason is that the cantilever structure formed by the fracture of the low key layer has a buffer effect on the working face, reducing the impact on the working face.

5. Conclusion

(1) Based on the engineering geological conditions of 61601 fully mechanized caving face in Longwanggou Coal Mine, a three-dimensional physical similarity model was established to carry out the experimental study on the migration law of grazing rock in fully mechanized working face with large mining height in real stress environment

(2) According to the experimental phenomenon of three-dimensional model, it is concluded that the migration law of mining-induced rock in 61601 working face: the breaking length of low key layer is greater than that of high key layer, and the number of periodic weighting is more frequent, which will produce obvious weighting phenomenon. The downward rotation movement and fracture subsidence of the rock layer lead to the displacement curve of the fractured rock block in the key layer increased in a "step" type

(3) Based on the analysis of displacement continuous monitoring results, the working face pressure is obtained: the displacement of measuring point increases suddenly for the first time when the working face advances to 90 cm, so the first weighting interval of 61601 working face is 90 cm. Subsequently, the displacement of measuring points changed significantly when the working face, respectively, advanced to 105 cm, 115 cm, 135 cm, 150 cm, 165 cm, 180 cm, 215 cm, and 240 cm. It was speculated that the periodic weighting occurred at the working face, which was consistent with the experimental phenomenon

(4) The average strain of fiber test in model test is proposed. The first weighting and periodic weighting laws of the working face are represented by the strain average degree, which are consistent with the experimental phenomena. The first weighting shows the first mutation peak in the average strain curve, and the periodic weighting shows the periodic mutation peak change of the strain average curve

Data Availability

The data used to support the findings of this study are available from the corresponding author upon request.

Conflicts of Interest

The authors declare that they have no known competing financial interests or personal relationships that could have appeared to influence the work reported in this paper.

Authors' Contributions

Jing Chai was responsible for the conceptualization and methodology. Zhicheng Tian was responsible for writing the original draft. Yibo Ouyang was responsible for data curation. Yongliang Liu was responsible for the validation and methodology. Dingding Zhang was responsible for the project administration. Jianfeng Yang was responsible for writing, review, and editing.

Acknowledgments

Thanks are due to funds supported by the Key Program of National Natural Science Foundation of China (No. 41027002). Many thanks are due to Professor Chai for the guidance of this paper.

References

[1] J.-H. Wang, "Key technology for fully-mechanized top coal caving with large mining height in extra-thick coal seam," *Journal of China Coal Society*, vol. 38, no. 12, pp. 2089–2098, 2013.

[2] P. K. Sarswat, P. Podder, Z. Zhang, and M. L. Free, "Autogenous acid production using a regulated bio-oxidation method for economical recovery of REEs and critical metals from coal-based resources," *Applied Surface Science Advances*, vol. 11, article 100283, 2022.

[3] Y. Wang, J. Mao, F. Chen, and D. Wang, "Uncovering the dynamics and uncertainties of substituting coal power with renewable energy resources," *Renewable Energy*, vol. 193, pp. 669–686, 2022.

[4] L. Xue, W. Zhang, Z. Zheng et al., "Measurement and influential factors of the efficiency of coal resources of China's provinces: based on bootstrap-DEA and Tobit," *Energy*, vol. 221, article 119763, 2021.

[5] J. Zhou, J. Zhang, J. Wang, F. Li, and Y. Zhou, "Research on nonlinear damage hardening creep model of soft surrounding rock under the stress of deep coal resources mining," *Energy Reports*, vol. 8, pp. 1493–1507, 2022.

[6] Y. Jianfeng, L. Haojie, and L. Li, "Fracturing in coals with different fluids: an experimental comparison between water, liquid CO_2, and supercritical CO_2," *Scientific Reports*, vol. 10, no. 1, article 18681, 2020.

[7] A. Çelik and Y. Özçelik, "Investigation of the efficiency of longwall top coal caving method applied by forming a face in horizontal thickness of the seam in steeply inclined thick coal seams by using a physical model," *International Journal of Rock Mechanics and Mining Sciences*, vol. 148, article 104917, 2021.

[8] C. Liu, P. Zhang, J. Shang et al., "Comprehensive research on the failure evolution of the floor in upper mining of deep and thick coal seam," *Journal of Applied Geophysics*, vol. 206, article 104774, 2022.

[9] C. Pan, B. Xia, Y. Zuo, B. Yu, and C. Ou, "Mechanism and control technology of strong ground pressure behaviour induced by high-position hard roofs in extra-thick coal seam mining," *International Journal of Mining Science and Technology*, vol. 32, no. 3, pp. 499–511, 2022.

[10] C. Zhu, J. Zhang, M. Li, Z. He, Y. Wang, and Y. Lan, "Effect mechanism of strata breakage evolution on stope deformation in extra- thick coal seams," *Alexandria Engineering Journal*, vol. 61, no. 6, pp. 5003–5020, 2022.

[11] H. Lv, Z. Cheng, and F. Liu, "Study on the mechanism of a new fully mechanical mining method for extremely thick coal seam," *International Journal of Rock Mechanics and Mining Sciences*, vol. 142, article 104788, 2021.

[12] J. Yu and D. Mao, "Status and countermeasures of roof management in China coal mines," *Coal Science and Technology*, vol. 45, no. 5, pp. 65–70, 2017.

[13] Z. Li, X. He, and L. Dou, "Control measures and practice for rock burst induced by overburden fracture in top-coal caving mining," *Journal of China University of Mining and Technology*, vol. 47, no. 1, pp. 162–171, 2018.

[14] J. Xu and J. Ju, "Structural morphology of key stratum and its influence on strata behaviors in fully-mechanized face with super-large mining height," *Journal of Rock Mechanics and Engineering*, vol. 30, no. 8, pp. 1547–1556, 2011.

[15] Y. Pan, "Integrated study on compound dynamic disaster of coal-gas outburst and rockburst," *Journal of China Coal Society*, vol. 41, no. 1, pp. 105–112, 2016.

[16] R. Gao, B. Huo, H. Xia, and X. Meng, "Numerical simulation on fracturing behaviour of hard roofs at different levels during extra-thick coal seam mining," *Royal Society Open Science*, vol. 7, no. 1, article 191383, 2020.

[17] X. Li, S. Chen, E. Wang, and Z. Li, "Rockburst mechanism in coal rock with structural surface and the microseismic (MS) and electromagnetic radiation (EMR) response," *Engineering Failure Analysis*, vol. 124, article 105396, 2021.

[18] B. Yu, J. Zhao, T. Kuang, and X. Meng, "In situ investigations into overburden failures of a super-thick coal seam for longwall top coal caving," *International Journal of Rock Mechanics & Mining Sciences*, vol. 78, pp. 155–162, 2015.

[19] H. Liu, T. Huo, Y. Liu, Z. Han, Z. Han, and W. Liang, "Study on the migration law of overlying strata on the working surface of large mining height in Y.C.W coal mine," *Geofluids*, vol. 2022, Article ID 6292783, 13 pages, 2022.

[20] H. P. Kang, Z. Zhang, and Z. Z. Huang, "Characteristics of roof disasters and controlling techniques of coal mine in China," *Safety in Coal Mines*, vol. 51, no. 10, pp. 24–33, 2020.

[21] J. Chai, Z. Ma, D. Zhang, Q. Yuan, and W. Lei, "Experimental study on PPP-BOTDA distributed measurement and analysis of mining overburden key movement characteristics," *Optical Fiber Technology*, vol. 56, article 102175, 2020.

[22] J. Chai, W. Lei, W. Du et al., "Experimental study on distributed optical fiber sensing monitoring for ground surface deformation in extra-thick coal seam mining under ultra-thick conglomerate," *Optical Fiber Technology*, vol. 53, article 102006, 2019.

[23] J. Chai, Y. OuYang, and D. Zhang, "Crack detection method in similar material models based on DIC," *Journal of Mining and Strata Control Engineering*, vol. 2, no. 2, pp. 74–84, 2020.

[24] Y. Jianfeng, L. Haojie, and L. Li, "Investigating the effect of confining pressure on fracture toughness of CO_2-saturated coals," *Engineering Fracture Mechanics*, vol. 242, article 107496, 2021.

[25] J. Chai, Y. L. Liu, and Q. Yuan, "Theory - technology and its application of optical fiber sensing on deformation and failure of mine surrounding rock," *Coal Science and Technology*, vol. 49, no. 1, pp. 208–217, 2021.

[26] F. Cui, C. Jia, and X. Lai, "Study on deformation and energy release characteristics of overlying strata under different mining sequence in close coal seam group based on similar material simulation," *Energies*, vol. 12, no. 23, article 4485, 2019.

[27] B. Yu, W. B. Zhu, R. Gao, and J. R. Liu, "Strata structure and its effect mechanism of large space stope for fully-mechanized sublevel caving mining of extremely thick coal seam," *Journal of China Coal Society*, vol. 41, no. 3, pp. 571–580, 2016.

[28] L. Kong, F. Jiang, S. Yang, J. Song, and C. Wang, "Movement of roof strata in extra-thick coal seams in top-coal caving mining based on a high precision micro-seismic monitoring system," *Journal of University of Science and Technology Beijing*, vol. 32, no. 5, pp. 552–558, 2010.

[29] J. Chai, Y. Qian, F. Wang, Q. Yuan, and D. Zhang, "An internal displacement measurement device for three dimensional model and its application," *Chinese Journal of Underground Space and Engineering*, vol. 12, no. S2, pp. 532–537, 2016.

[30] Q. Zhang, K. Yang, L. Yuan, and C. Duan, "Experimental study on deformation and collapse characteristics of two stope belts based on continuous displacement monitoring," *4Advanced Engineering Sciences*, vol. 51, no. 3, pp. 36–42, 2019.

[31] Z. X. Li, G. Y. Hou, T. Hu, T. C. Zhou, and H. L. Xiao, "Study on establishing and testing for strain transfer model of distributed optical fiber sensor in concrete structures," *Optical Fiber Technology*, vol. 61, article 102430, 2021.

[32] W. G. Du, J. Chai, D. Zhang, Y. Ouyang, and Y. Liu, "Study on quantitative characterization of coupling effect between mining-induced coal-rock mass and optical fiber sensing," *Sensors*, vol. 22, no. 13, article 5009, 2022.

[33] J. Xu, P. Wu, and W. Zhu, "Computer realization of judging key stratum," *Ground Pressure and Strata Control*, vol. 4, pp. 29–31, 2000.